Journal of Information Systems Engineering and Management
2025, 10(48s)
e-ISSN: 2468-4376
https://www.jisem-journal.com/

Research Article

Development of an Optimized PID Control Strategy for PV-Integrated Microgrids in Modern Power System

Muhamad Nabil Bin Hidayat[1], Naeem Hannoon*[2], Wan Noraishah Wan Abdul Munim[3], Rahimi Baharom[4]
[1,2,3,4]*School of Electrical Engineering, College of Engineering, Universiti Teknologi Mara, Shah Alam, Malaysia.*

ARTICLE INFO

Received: 29 Dec 2024
Revised: 15 Feb 2025
Accepted: 24 Feb 2025

ABSTRACT

This work presents the design and analysis of an optimized Proportional-Integral-Derivative (PID) controller for photovoltaic (PV)-based microgrids integrated into power systems. Conventional PI controllers often suffer from issues such as prolonged oscillation time, high amplitude responses, excessive overshoot, and persistent steady-state errors—particularly during fault conditions in PV microgrids. To address these limitations, this study aims to introduce and evaluate an optimized PID controller that enhances system responsiveness and improves stability under both DC and AC fault conditions. The proposed controller is designed to maintain current regulation stability during outages caused by unsymmetrical faults, considering scenarios with varying load demands and transmission line lengths. A PI controller is implemented within the current regulation loop, and the gains of the DC/DC boost converter are tuned using a trial-and-error approach to ensure stable current flow during faults. Comprehensive stability and performance evaluations are conducted using Bode plots and pole-zero mapping techniques in MATLAB/Simulink to validate the effectiveness of the control strategy. The performance of the optimized PID controller is compared against a conventional PID controller under multiple scenarios. The results demonstrate improved dynamic response, reliability, and system robustness. Overall, the proposed control design, tuning methodology, and analytical validation under unsymmetrical fault conditions confirm its suitability for enhancing PV-based microgrid operations.

Keywords: PV; PID Controller; PV Microgrid; Fault MATLAB/Simulink; Bode Plot Analysis; Pole-Zero Analysis; DC Fault; Unsymmetrical AC Fault

INTRODUCTION

The diminishing availability of conventional energy sources such as natural gas, fossil fuels, and oil has become a growing concern due to the widening gap between energy generation and consumption, leading to a global energy crisis. This crisis has raised significant concerns about energy security and the risk of shortages for consumers, driven by increasing net load demand. As a result, non-conventional energy sources have emerged as environmentally beneficial alternatives [1]. Among various renewable energy sources, solar energy has shown the most promise due to its abundance and the ability to be efficiently converted into electricity using photovoltaic (PV) technology—without contributing to pollution [2].

PV modules have become a key component in alternative energy generation, recognized for their cost-effectiveness, long lifespan, low maintenance, minimal emissions, and ease of deployment [3]. In a grid-connected PV system, the architecture resembles that of a traditional power grid, comprising interconnected power generation stations, long-distance transmission lines, and substations that distribute power to consumers. Such systems typically include a series of PV modules arranged in arrays—the fundamental power conversion units of the generator system. These modules are cascaded with a DC/DC boost converter to regulate and elevate the DC voltage before interfacing with a DC/AC inverter, which then connects to the grid via transformers [4].

Microgrids have gained considerable attention in recent years as viable alternatives to conventional power systems, offering enhanced efficiency and reduced environmental impact. These systems are generally deployed to support the main power grid, often located on the same site and connected to the low-voltage distribution network. While individual microgrid components are well-understood, the behavior of an integrated system with multiple energy sources remains complex and somewhat unpredictable [5]. This underscores the importance of advanced power

Research Article

converter technologies, which contribute significantly to improving the efficiency of Maximum Power Point Tracking (MPPT) and overall system performance. Furthermore, variable load conditions can be addressed by minimizing distribution losses and optimizing the utilization of components such as transformers and transmission lines [6].

The Voltage Source Converter (VSC), widely used in such systems, is commonly controlled using classical methods such as the Proportional-Integral-Derivative (PID) controller. However, these conventional techniques often require an exact mathematical model and detailed tuning of parameters [7]. Despite the availability of newer theories, the PID controller remains widely used in industrial process control and power electronics due to its simplicity and proven performance [8]. The three components of the PID controller help achieve a desirable system response by managing overshoot, settling time, and steady-state error [9]. Nonetheless, the effectiveness of PID control depends heavily on proper tuning, which can be challenging and often requires advanced optimization methods [10].

Classical control methods typically fail to accommodate rapid fluctuations in load demand or the dynamic behavior of power electronic systems. Advanced control techniques are required to improve steady-state and transient performance under varying operational conditions [11]. Several existing studies have focused on addressing individual challenges in solar energy systems using PID controllers [10]. Motivated by these limitations, this study proposes an optimization-based approach to PID control aimed at enhancing microgrid stability under fault conditions, especially in scenarios involving high load demand and varying transmission line lengths.

Conventional PID controllers often fall short in handling the intermittent and unpredictable nature of renewable energy sources like solar power. Their inability to adapt to sudden changes in operating conditions can significantly degrade system performance [12]. In weak grid systems, they may also fail to accurately track real and reactive power without overshoot or undershoot, necessitating more complex control strategies for reliable operation [13]. Additionally, the presence of steady-state errors when using traditional PID controllers in PV-connected microgrids results in reduced system stability and accuracy.

While widely adopted for maintaining stable output voltage and current, conventional PID controllers are limited in their ability to manage system errors effectively, often leading to interference and inefficiencies. Therefore, this study aims to introduce, test, and validate an optimized PID controller specifically designed for PV-based microgrids. This optimized approach is expected to improve system response speed and enhance stability during DC and AC fault conditions. The PID controller is seen as a vital component in stabilizing the system, particularly during outages caused by increased load demand or varying transmission line lengths.

In this study, a Proportional-Integral (PI) controller is embedded within the current regulator to enhance current performance during fault conditions. The PI controller is selected due to its suitability for controlling VSCs in connecting PV panels to three-phase electrical networks. Its role is to reduce rise time and steady-state error, thereby improving system performance. Additionally, the gain of the DC/DC boost converter is fine-tuned to evaluate system behavior under DC fault scenarios. To assess system stability, Bode plots and Pole-Zero diagrams are derived from the controller's response. The simulation and analysis are conducted using MATLAB/Simulink, with the ultimate goal of designing a system that can be practically implemented under real-world fault conditions.

PI Controller

A Proportional-Integral (PI) controller combines the functionalities of both proportional and integral control modes to produce a more effective control output [14]. It is commonly used in voltage and current regulation, particularly in photovoltaic (PV) systems connected to microgrids. In a closed-loop control system, the feedback loop continuously monitors the output and compares it to the reference input to generate an error signal—the difference between the desired and actual output.

The proportional control component responds to the present error, helping to reduce both the rise time and steady-state error. On the other hand, the integral control component responds to the accumulated error over time, aiming to eliminate any residual steady-state error that persists after the proportional action. Together, these modes allow the PI controller to improve system stability and dynamic performance, making it suitable for real-time control applications in PV-based microgrid environments.

The equation of PI combination controller is stated in Equation (1).

Journal of Information Systems Engineering and Management
2025, 10(48s)
e-ISSN: 2468-4376
https://www.jisem-journal.com/

Research Article

$$K_p + \frac{K_i}{s} = K_p \frac{(s+\frac{K_i}{K_p})}{s} \quad (1)$$

Where Kp is proportional gain and Ki is the integral gain. The ultimate reason for using PI controller is due to the simpler executions rather than using PID controller. PID controllers are more complex controllers and require tuning of three parameters even though it can reduce the overshoot due to the predictive action. PI controller is believed to improve the stability of the system as well as give the faster response to the disturbance and reduce the steady state error [15]. While the PI controller is easier to design and works well for systems with slower dynamics where precision is not as critical, it excels especially in terms of stability, response time, and handling transient responses. The key distinction is the derivative term in the PID controller, which offers superior performance in dynamic systems, but PI controller works the best in simple system [16].

MODEL DESCRIPTION

Throughout this entire simulation, there are a few steps that must be taken into consideration to fulfil the objectives of this study.

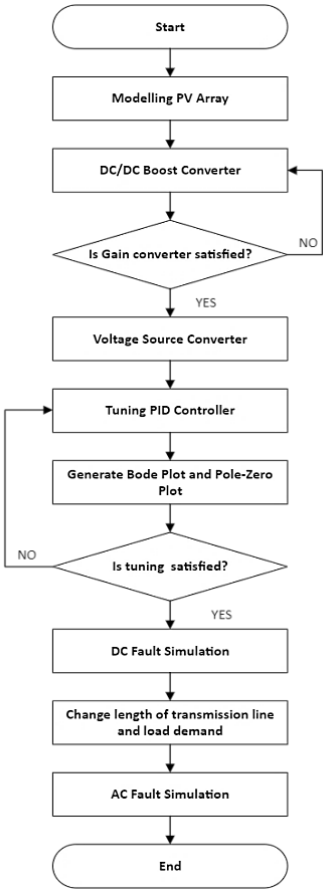

Figure 1: Flowchart of Designing PID Controller

First step, designing the PV array based on standard test conditions (stc). Then, the gain controller in DC/DC booster is tuned to specific value to obtained better performance to the system. Once the gain for the controller has been satisfied, VSC's role will be played as the PID controller is installed inside VSC converter. By using trial and error method of tuning for PID controller, results of Bode Plot and Pole-Zero plot will be the reference for comparative analysis to get the optimized value for the system. The steps will be repeated until the exact value is received before continuing for DC fault simulation result. As for the next steps, since there will be two situations for this study, the variable will be changed based on the situations before the last step which are getting the AC fault simulation result for unsymmetrical fault that involve single line to ground, double line to ground and line-to-line fault.

Journal of Information Systems Engineering and Management
2025, 10(48s)
e-ISSN: 2468-4376
https://www.jisem-journal.com/

Research Article

System Description

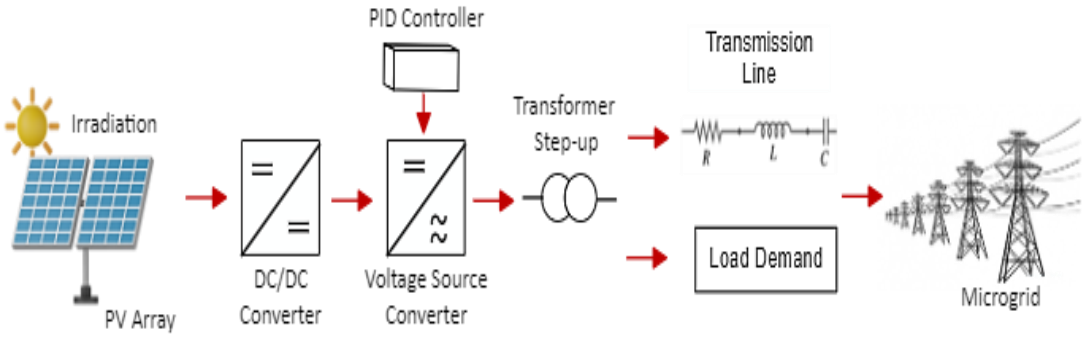

Figure 2: Shows structure of PV with microgrid connected

The simulation process involves a series of structured steps aimed at achieving the objectives of this study. The first step is the design of the photovoltaic (PV) array, configured according to Standard Test Conditions (STC). Following this, the gain of the DC/DC boost converter is tuned to specific values in order to improve system performance. Once satisfactory gain values are obtained, the Voltage Source Converter (VSC) is integrated into the system, where the PID controller is implemented within the VSC.

Using a trial-and-error tuning method, the controller is adjusted based on system response, and the results are analyzed using Bode plots and Pole-Zero plots. These analyses are used as references to fine-tune the controller parameters until an optimized configuration is reached. Once optimized, the simulation proceeds to test the system's behavior under DC fault conditions.

This study evaluates two different scenarios:

Long transmission line with high load

Short transmission line with low load

Before proceeding to AC fault simulations, system parameters such as transmission line length and load demand are adjusted according to the scenario being tested. In the final step, the system is subjected to AC fault simulations, focusing on unsymmetrical faults, including single line-to-ground (SLG), double line-to-ground (DLG), and line-to-line (LL) faults.

The system configuration, including the placement of the PI controller within the VSC for a PV microgrid under varying transmission lines and loads, is illustrated in Figure 2. In this study, four PV arrays are connected in parallel to meet the desired power output. Each array is configured under 1,000 W/m² irradiance (under normal incidence) and tested at two temperature settings: 25°C and 45°C. The average power output from each array is approximately 100 kW, with a duty cycle of 0.5.

A DC/DC boost converter is connected to the PV array to enhance output voltage, with an embedded Maximum Power Point Tracking (MPPT) algorithm that dynamically adjusts the operating point of the PV modules. The PID controller within the VSC is integrated alongside a Phase-Locked Loop (PLL), a current regulator, and a voltage regulator. The PLL ensures synchronization between the converter output and the grid in terms of frequency and phase, while the current regulator, as aligned with the study's objectives, plays a central role in maintaining system stability.

The PV stations are then connected to the microgrid via three-phase transformers rated at 260 V/25 kV (Δ/Y configuration). The simulation considers two distinct scenarios:

Long transmission line: 300 km with a high load of 50 MW

Short transmission line: 0.5 km with a low load of 0.5 kW.

Journal of Information Systems Engineering and Management
2025, 10(48s)
e-ISSN: 2468-4376
https://www.jisem-journal.com/

Research Article

PV Array

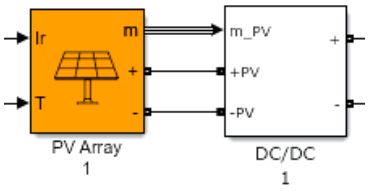

Figure 3: Show PV array in MATLAB/Simulink

PV stations use many modules linked in series to get the necessary voltage level. To provide the necessary power capacity, a PV array is formed by connecting many PV strings in parallel. The DC/DC boost converter connects each PV array to maximize power output despite variations in solar irradiation. The PV arrays are attached in parallel to the main DC/AC converter to manage active power to the grid and obtain the desired reactive power [17]. There are 64 parallel strings with 5 series connected modules per strings per PV array where 256 parallel strings and 20 series in total. Fig. 4 shows the equivalent circuit of solar cells.

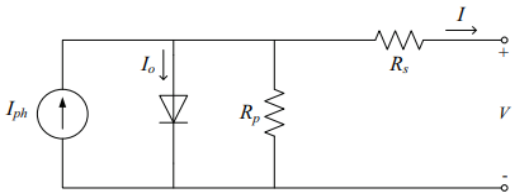

Figure: 4 Equivalent circuit of solar cell

An equivalent circuit of solar cell can be represented by (2) where Iph is the solar generated current and Io is the diode saturation current. Vt shows the thermal voltage of the array (NskTa/q) consisting of Ns, which is the number of cells connected in series, q=1.6 x10-19 C stands for the electron charge, k meanwhile is the Boltzmann's constant, 1.38 x 10-23 J/K, a represents the diode ideal factor, Rs and Rp are the series and parallel resistance respectively. The photocurrent, Iph influenced by solar irradiance (1000 W/m²) and temperature (25°C) can be calculated as in Equation (3) The diode saturation current can be calculated based on the change of the cell temperature in equation (4). Then, the reverse saturation current at a reference temperature and irradiance is denoted by Irs, whereas Tr and T represent the 298K reference temperature and operating temperature in k, respectively. Eg = 1.13 eV represents the band energy gap of the semiconductor utilized in the cell. Equation (5) expresses the reverse saturation current (Irs). The Voc in equation (5) represents PV cell open circuit voltage.

$$I = Iph - Io\left[\exp\left(\frac{V+RsI}{NskTa/q}\right) - 1\right] \quad (2)$$

$$Iph = \frac{\lambda}{1000}[Isc + \gamma Isc\,(T - Tstc)] \quad (3)$$

$$Io = Irs\left(\frac{T}{Tr}\right)^3 exp\left[\frac{qEg}{ak}\left(\frac{1}{Tr} - \frac{1}{T}\right)\right] \quad (4)$$

$$Irs = \frac{Isc}{\exp\left(\frac{Vocq}{NskTa}\right)-1} \quad (5)$$

The parameter for calculations can be obtained from the provided datasheet in Table 1. Table 1 shows the specifications of PV array for this study which is Sunpower SPR-315E-WHT-D (315W) model from MATLAB/Simulink selection.

Table 1: Sunpower SPR-315E-WHT-D photovoltaic Module Specifications

Model Type	Monocrystalline Silicon
Maximum Power (Pmax)	315.0 W
Open Circuit Voltage (Voc)	64.6V
Short Circuit Current (Isc)	6.14 A

Journal of Information Systems Engineering and Management
2025, 10(48s)
e-ISSN: 2468-4376
https://www.jisem-journal.com/

Research Article

Voltage at maximum power point Vmp (V)	54.7 V
Current at maximum power point Imp (V)	5.76A
Temperature coefficient of Voc (%/deg.C)	-0.2727 %/deg.C
Temperature coefficient of Isc (%/deg.C)	0.061743 %/deg.C

The electrical characteristics of PV array can be simulated based on the temperature which are 25 degrees Celsius and 45 degrees Celsius. Fig. 5 shows the comparison for I-V and P-V curves. It is shown that the short circuit current at 25 degrees Celsius gives a better generations capability rather than 45 degrees Celsius. The peak of the P-V curve indicates that solar array at 25 degrees Celsius manages to deliver more power at lower temperatures. Therefore, the temperature of 25 degree Celsius has been chosen.

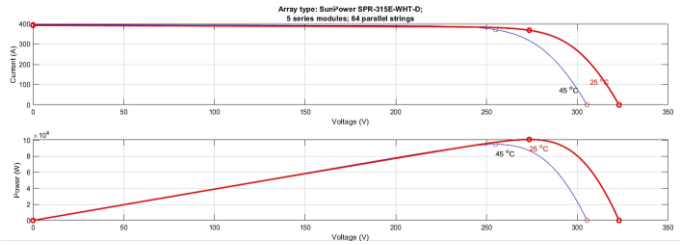

Figure 5: I-V and P-V curve

DC/DC Converter

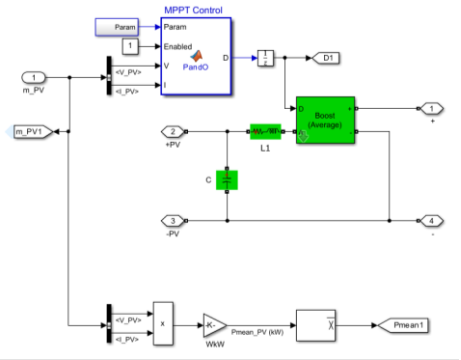

Figure 6: Shows component inside DC/DC Converter

Since the output voltage of PV array is very low, step-up converter is one of the crucial equipment to be installed which are used to increase the level of PV voltage. A DC-DC converter may operate as a switching mode regulator, converting unrestrained DC voltage to regulated DC output voltage. Typically, PWM and switching devices are used to regulate fixed frequencies. The boost converter has two modes. When the switch is closed in Mode I, the current progressively rises via the inductor, but diode D remains off. When the switch is opened in Mode II, current flows via the inductors, diodes, capacitors, and loads [18]. As for these studies, the duty cycle is approximately 0.5 for each of the converters. The switch has a duty ratio, D which is defined as

$$D = \frac{ton}{ton+toff} = \frac{ton}{T} \qquad (6)$$

The relation between the output and input voltage of the converter is as follow

$$\frac{Vo}{Vs} = \frac{1}{1-D} \qquad (7)$$

The MPPT strategies are also pivotal in conversion of PV array system since the intensity of solar irradiation varies with the time where MPPT can detect the maximum output power under variation of solar irradiance. Therefore,

Journal of Information Systems Engineering and Management
2025, 10(48s)
e-ISSN: 2468-4376
https://www.jisem-journal.com/

Research Article

the objectives of MPPT technique are to regulate the boost converter controller to ensure the PV array may operate at the peak of power point [17]. During the simulation, the gain for boost converter has been changed to the most optimal value which is 0.02 to obtain the best performance to the system during outages by using comparative method.

VSC Controller and PI Controller Tuning Methodology

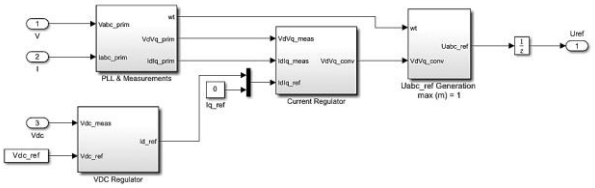

Figure 7: Voltage Source Converter

The Voltage Source Converter (VSC) controller utilized in this study refers to a power electronic control technique designed to manage and regulate system operations effectively. In photovoltaic (PV) systems, the VSC plays a crucial role by converting the DC voltage output from the PV array into AC voltage using semiconductor switching devices. The VSC controller is capable of controlling both the magnitude and phase angle of the output voltage, making it essential for maintaining synchronization and stability within the microgrid.

In this study, PID controllers are implemented within both the current regulator and the voltage regulator blocks of the VSC. The PID controller for the voltage regulator is tuned automatically using MATLAB/Simulink's built-in system specification tools. Meanwhile, the current regulator's PID controller is manually tuned through an empirical (trial-and-error) method to meet the specific performance objectives of this research.

Location and Function of the PI Controller in the VSC

Refer to Fig. 8 for the placement of the PID controller within the VSC system.

Inside the current regulator, a Proportional-Integral (PI) controller is employed due to its balance of simplicity and effectiveness in regulating current. This two-mode controller includes:

A Proportional (P) component that responds to the present error and improves the response speed and transient behavior, and

An Integral (I) component that addresses steady-state errors by integrating past errors over time.

The PI controller is optimized to enhance system response in terms of settling time, overshoot, and steady-state error. The trial-and-error tuning method used involves incrementally testing a range of values—starting from low to high—for the integral gain while monitoring system performance, particularly the quality of the current waveform.

After iterative testing and analysis, the optimal PI controller gains were determined to be:

Proportional gain (Kp): 0.3

Integral gain (Ki): 0.02

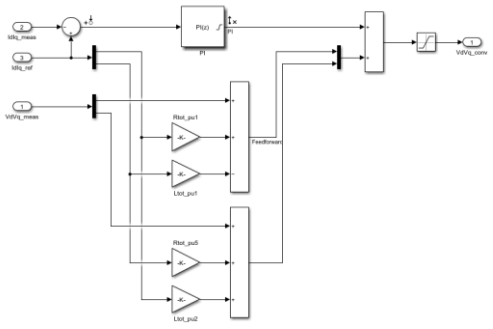

Figure 8: Location of PID controller inside VSC

Journal of Information Systems Engineering and Management
2025, 10(48s)
e-ISSN: 2468-4376
https://www.jisem-journal.com/

Research Article

The Model Linearizer App in MATLAB/Simulink was used to set the PI controller parameters. In this setup:

Input perturbation represents the current measurement input to the PI controller. Open-loop output selection is made after the PI controller block to enable linear system analysis.

To assess the controller's stability and dynamic performance, Bode plots and Pole-Zero plots were generated. These tools helped determine whether the chosen PI controller values provide a stable response and meet the desired system performance criteria.

RESULT ANALYSIS

In this part, a few stabilities analysis have been done to ensure the value that has been chosen met the objectives of this project. Although this study has been used try-and-error method, stability test also has been conducted to observed whether the chosen value is able to improve the current during outages. The steps have been taken a few times before deciding the optimized value for this study. The AC fault has been set to occur for 0.02 seconds from 1 seconds to 1.02 seconds. Table 2 and 3 shows the parameter that has been used to obtain all the results.

Table 2: Shows the parameter of Gain in DC/DC Booster, Kp and Ki of the Controller

	DC/DC Gain	Kp	Ki
Conventional	0.02	0.3	7
Optimized	0.02	0.3	0.02

Table 3: Shows the parameter of DC fault, length of transmission line and load

	Kp	Ki	Length of Transmission Line	Load
Situation I	0.3	0.02	300 km	50MW
Situation II	0.3	0.02	0.5 km	5kW

Controller Stability Analysis

Bode Plot Analysis

Bode plot analysis is vital for the design and tuning of PID controllers, especially in PV-connected microgrids. It gives crucial information on the system's frequency response, which is necessary for assuring stability, optimizing performance, and improving the interaction between the PV system and the microgrid. The stability in margin derived and achieved from bode plot may help to identify whether the PID Controller system will remain stable under the operating conditions which is fundamental for preventing malfunctions in PV system with microgrid connected. By doing this bode plot analysis, the PID controller may ensure that it can meet the design specifications and performance as expected in real-world scenarios.

Fig. 9 shows the magnitude part of the bode plot for the comparison between conventional and optimized PI controller. The proposed controller has a lower magnitude gain at higher frequencies, which indicates better attenuation of high-frequency noise and disturbances. Meanwhile, lower gain at high frequencies for conventional controller is generally desirable for system stability as it reduces the amplification of high-frequency signals that could potentially cause instability or oscillations. The proposed controller has a smoother roll off at higher frequencies, which suggests a more well-damped system response compared to the conventional controller, which exhibits a sharper roll off.

As for the phase part of the bode plot for Fig. 10, optimized controller has a higher phase margin compared to the conventional controller. Phase margin is a measure of how much phase lag the system can tolerate before becoming unstable, and a higher phase margin generally indicates better stability. Phase margin is determined by the frequency at which the phase curve crosses the -180° line. The farther this crossing point is from the 0 dB gain crossover frequency, the higher the phase margin and the better the stability. Optimized controller crosses the -180° line at a

Journal of Information Systems Engineering and Management
2025, 10(48s)
e-ISSN: 2468-4376
https://www.jisem-journal.com/

Research Article

lower frequency compared to the conventional controller. This implies that the optimized controller has a higher phase margin, which can be said to a better stability of the system.

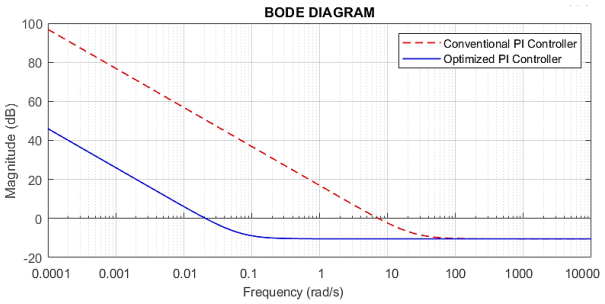

Figure 9: Bode Plot Diagram for Magnitude

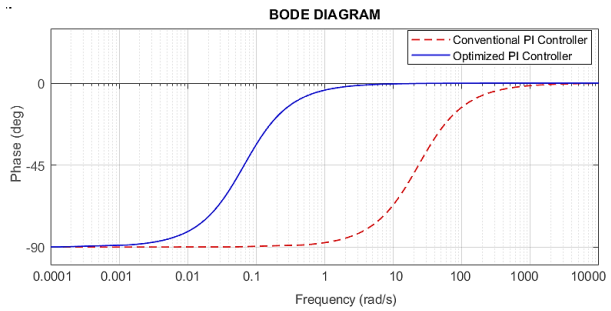

Figure 10: Bode Plot Diagram for Phase

Pole-Zero Plot Analysis

This analysis is being conducted to determine the stability of the closed-loop control system which is important to ensure the reliability of the system. By identifying the location of system's pole which is the roots of the denominators polynomial, and zero for roots of numerator polynomial, the stability can be reassured. Poles and Zeros will influence the system's transient response characteristic such as rise time, settling time, overshoot an the steady-state error. Table 4 shows the actual value of location for pole and zero where it lies on the plane.

Table 4: Location of Pole and Zero on the plane.

	Zero	Dampin g	%OS	Frequency
Conventional	0.99 8	1	0	23.4
Optimized	1	1	0	0.0667

Conventional controller has a single pole located at 0.998 on the real axis, entirely in the right half plane. The presence of a pole in the RHP implies that the system is unstable. Furthermore, the pole's location far from the imaginary axis indicates that the system's response will be heavily damped, with a non-oscillatory but growing (unstable) behavior. Meanwhile the optimized controller has a single pole located at 0.1 + j0.0667 in the complex plane. Since the pole lies in the RHP, this indicates that the system is marginally stable. The pole's location close to the imaginary axis suggests a lightly damped system response with a possibility of sustained oscillations.

Situation 1: Long Transmission Line & High Load

DC Fault Analysis

Journal of Information Systems Engineering and Management
2025, 10(48s)
e-ISSN: 2468-4376
https://www.jisem-journal.com/

Research Article

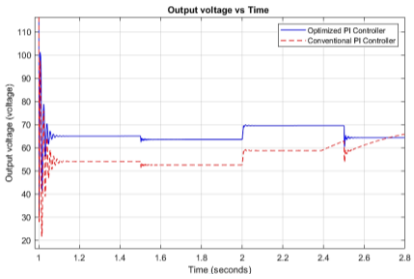

Figure 11: Time Series Plot

Figure 12 illustrates that the optimized PI controller achieves a shorter oscillation time, indicating a faster transient response when compared to the conventional PI controller. Specifically, the optimized controller is able to dampen oscillations within approximately 1.6 seconds, whereas the conventional controller continues oscillating until around 2.2 seconds, finally reaching steady state by 2.4 seconds.

In terms of overshoot, the conventional controller exhibits a peak response that reaches 100% of the steady-state value, which is significantly higher than that of the optimized controller, which shows an overshoot of approximately 80%. A high overshoot is generally undesirable as it can lead to system instability or additional stress on system components. Both controllers eventually settle at a steady-state output voltage between 62V and 64V after the transient oscillations subside. However, the optimized PI controller not only reduces the overshoot and settling time but also improves the system's resilience to disturbances and lowers the risk of instability.

In conclusion, the optimized PI controller offers superior dynamic performance, making it a more reliable choice for maintaining system stability in the presence of disturbances or faults.

AC Fault Analysis

Single Line to Ground

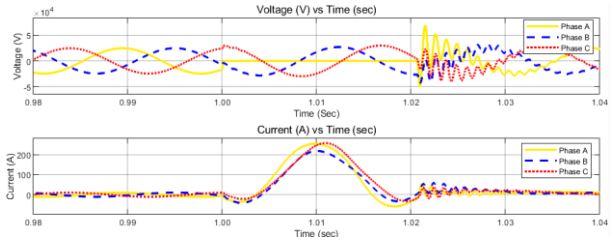

Figure 12. Conventional controller for single line to ground fault

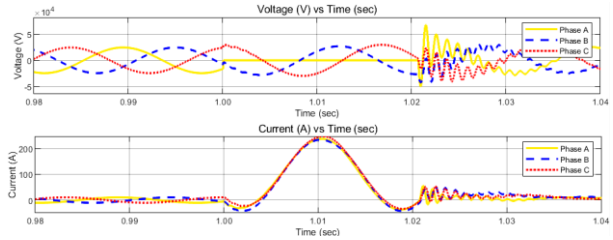

Figure 13. Optimized controller for single line to ground fault

The chosen phase for this part is phase A when the fault occurs, voltage will drop while the current will be high for 0.02 seconds. Each controller observes to have overshoot. The peak current for conventional controller is 284.0A with different values of other phases which are 217.0A and 256.0A for phase B and C respectively. Optimize controllers have the same value for phase A, phase B and phase C which is 235.1A that is lower than conventional controller.

Double Line to Ground

Journal of Information Systems Engineering and Management
2025, 10(48s)
e-ISSN: 2468-4376
https://www.jisem-journal.com/

Research Article

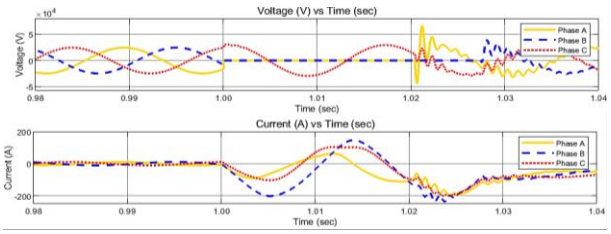

Figure 14. Conventional controller for double line to ground fault

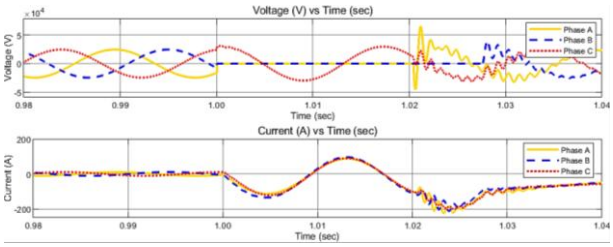

Figure 15: Optimized controller for double line to ground fault

As for this part, phase A and phase B have been chosen to shut down the voltage for the system. As for conventional controllers, the value is 57.05A, 150.0A and 99.0A for each phase respectively. Observed that the current drop occurs after 0.02seconds fault for 0.008s which makes the current -196.08A. Meanwhile optimized controller gives the same value of 90.15A for the three phases. There is also a current drop from -100A to -221A for 0.015 seconds before the current return to actual current.

Line to Line

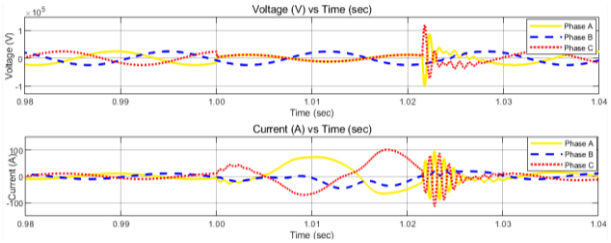

Figure 16: Conventional controller for line-to-line fault

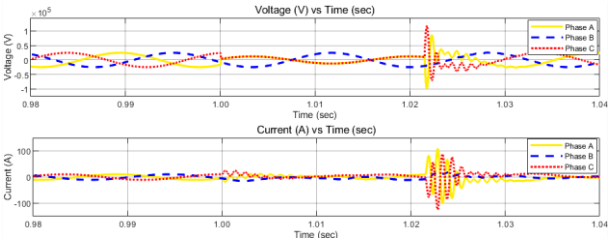

Figure 17: Optimized controller for line-to-line fault

When a fault occurs at phase A and phase C, voltage for both phases will become zero. Conventional controllers have an overshoot between 1.00 seconds till 1.02 seconds where phase A is 70 A while phase C is 100A. Phase B also become unstable based on Fig.17 the current drops from 0.0A to approximately -40.0A. An optimized controller gives much better stability to the current for the system. When outages occur, the current is stable yet there are disturbances have been observed for 0.004 seconds where the value for phase A is 106.0A and phase C is 62.0A

Situation II: Short Transmission Line & Low Load

DC Fault Analysis

Journal of Information Systems Engineering and Management
2025, 10(48s)
e-ISSN: 2468-4376
https://www.jisem-journal.com/

Research Article

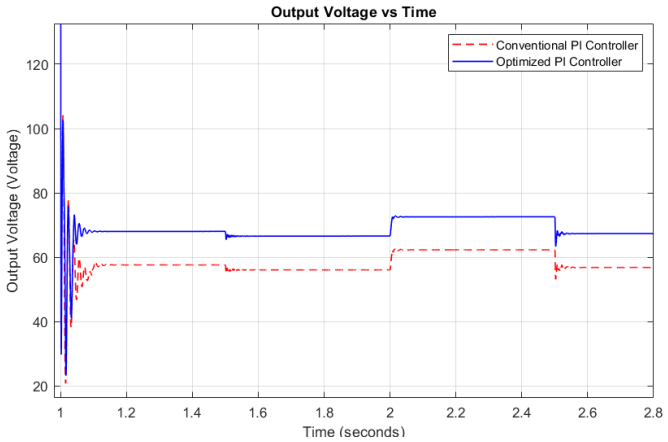

Figure 18: Time Series Plot

When DC fault occurs at the PV array, installing the PI controller dampens out the oscillation quicker where it is subsiding around 1.8 seconds while conventional controller's oscillation persists a prolonged duration where it is lasting beyond 2.6 seconds. The presence of overshoot around 1.4 seconds records for conventional controller is significant where it is approximately 100% of the maximum output voltage. While for optimized controller, the peak overshoot occurs at approximately 80% of the maximum output voltage around 1.2 seconds. After observing, the steady-state error appears to settle at the same value of steady state where it is approximately 62% to 64% of the maximum output voltage after the oscillation has subsided.

AC Fault Analysis

Single Line to Ground

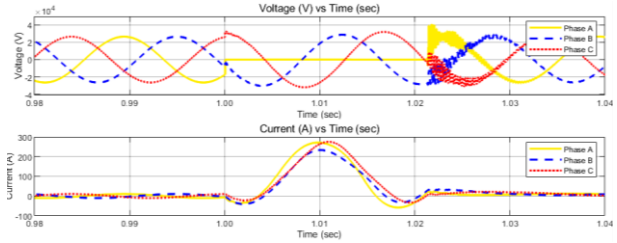

Figure: 19 Conventional controller for single line to ground fault

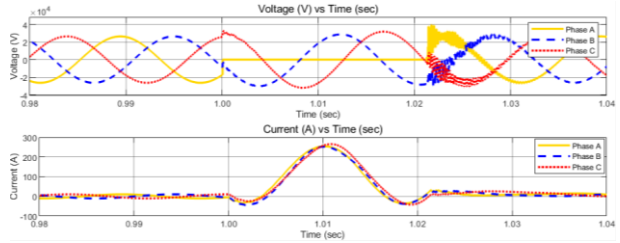

Figure 20: Optimized controller for single line to ground fault

Conventional controller when fault at phase A occurs makes the uneven value for the 3-phase current where phase A and phase C may reach 272.4A at peak while phase B recorded for 232.8 A at peak. After tuning an integral part of PI controller, the peak for 3-phase current is observed to be approximately the same at peak value. The value that has been recorded is 249.1A for phase A and B while phase C becomes 265.2A. Therefore, optimized controller helps in reducing an overcurrent situation by 8.45% for single line to ground fault for specifically phase A

Double Line to Ground

Journal of Information Systems Engineering and Management
2025, 10(48s)
e-ISSN: 2468-4376
https://www.jisem-journal.com/

Research Article

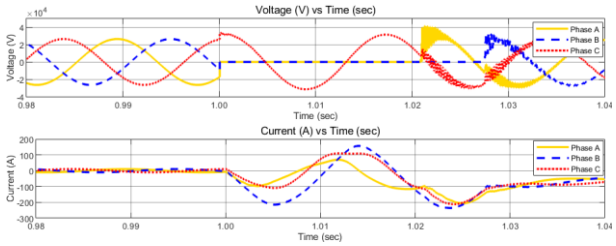

Figure 21: Conventional controller for double line to ground fault

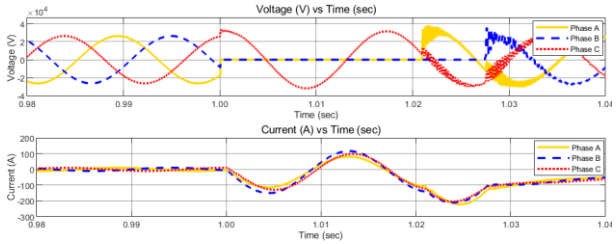

Figure 22: Optimized controller for double line to ground fault

Outages have happened at phase A and phase B with the recorded value of 69.18A, 155.0A and 107.0A for conventional controller's phase respectively before the current return to its actual value. Optimized controller happens to reduce the value of current for phase B which is 110.2A and C which is 93.5A meanwhile for phase A, the current higher compared to conventional which is 78.4A. There is a current drop of 0.008 second after outages happen with recorded value of -196.9A for phase A and -233.9A for phase B and C for conventional controller. There are also current drops for optimized controller but the value for every phase is better than conventional controller.

Line to Line

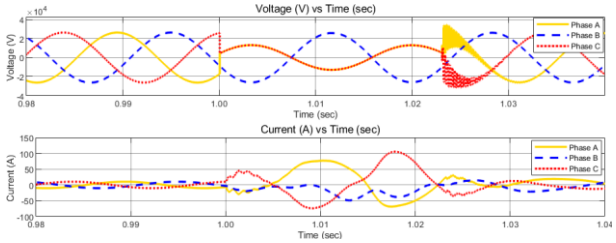

Figure 23: Conventional controller for line-to-line fault

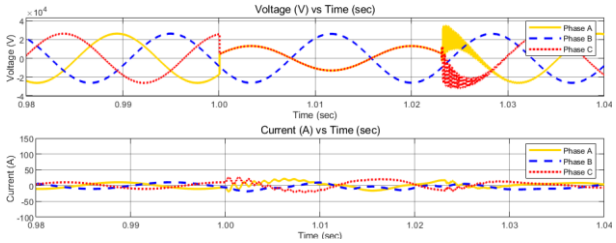

Figure 24: Optimized controller for line-to-line fault

Based on Fig.24 current shows the unstable result since phase A become 74.9A and phase C become 104.2A while current at phase B will drop to maximum at -50.0A. After optimizing the PI controller, current becomes stable even though there is presence of disturbance with the same amount of current flow before outages occur. This indicates optimized PI controller helps in maintaining that stability of the system especially for current part.

CONCLUSION

Summarize of Project

In this paper, a study was conducted to design and analyze an optimized PI controller for a PV microgrid connected

system, developed using MATLAB/Simulink. A comparative approach was employed to evaluate the differences between a conventional and an optimized PI controller under DC faults and unsymmetrical AC faults. During stability tests, the proposed controller exhibited a smoother roll-off at higher frequencies, indicating a well-damped system response compared to the conventional controller. The proposed controller also achieved a positive phase margin, signifying enhanced system stability.

In the case of DC faults, the optimized controller demonstrated faster transient response, with oscillations dampening more quickly and exhibiting lower peak overshoots compared to the conventional controller. During AC faults, it maintained more balanced currents and ensured quicker recovery times. The controller's effectiveness was consistently demonstrated across both long and short transmission line configurations, under varying load conditions.

By offering faster response times, reduced oscillations, and improved current control under diverse fault conditions, the optimized PI controller significantly enhanced the microgrid's stability and reliability. These results validate the controller's ability to improve PV microgrid performance, particularly during outages and high current demand, thereby contributing to stronger and more efficient renewable energy integration in power systems.

Future Recommendation

For future improvements, researchers could explore actual tuning methods such as Ziegler-Nichols, AMIGO, or Cohen-Coon, and compare their effectiveness with the current optimization techniques. Additionally, integrating Artificial Intelligence-based optimization techniques, such as Genetic Algorithms (GA) or Particle Swarm Optimization (PSO), could further enhance current control performance. Furthermore, adjusting the grounding resistance during AC faults could contribute to better current regulation, potentially yielding significant improvements in system stability and performance

REFERENCES

[1] R. K. Rai, M. Dubey, M. Kirar, and M. Kumar, "Analytical Analysis of Solar PV Module Using MATLAB," 2022 IEEE International Students' Conference on Electrical, Electronics and Computer Science, SCEECS 2022, pp. 1–6, 2022, doi: 10.1109/SCEECS54111.2022.9741019..

[2] N. El Hichami, A. Abbou, S. E. Rhaili, A. Ziouh, and S. Marhraoui, "Grid connected photovoltaic system using a fuzzy logic control approach," 2018 IEEE 59th Annual International Scientific Conference on Power and Electrical Engineering of Riga Technical University, RTUCON 2018 - Proceedings, pp. 1–5, 2018, doi: 10.1109/RTUCON.2018.8659872.

[3] K. Kachhiya, "MATLAB / Simulink Model of Solar PV Module and MPPT Algorithm," National Conference on Recent Trends in Engineering & Technology, no. May, p. 5, 2011.

[4] L. W. A. Badi, Z. Zakaria, A. H. M. Nordin, and R. F. Mustapa, "Unbalanced faults analysis in grid - Connected PV system," Conference Proceeding - 2014 IEEE International Conference on Power and Energy, PECon 2014, pp. 360–365, 2014, doi: 10.1109/PECON.2014.7062471..

[5] G. Bayrak and M. Cebeci, "Grid connected fuel cell and PV hybrid power generating system design with Matlab Simulink," Int J Hydrogen Energy, vol. 39, no. 16, pp. 8803–8812, 2014, doi: 10.1016/j.ijhydene.2013.12.029.

[6] D. Reddy and S. Ramasamy, "A fuzzy logic MPPT controller based three phase grid-tied solar PV system with improved CPI voltage," 2017 Innovations in Power and Advanced Computing Technologies, i-PACT 2017, vol. 2017-Janua, pp. 1–6, 2017, doi: 10.1109/IPACT.2017.8244953.

[7] M. A. Akcayol, "Application of adaptive neuro-fuzzy controller for SRM," Advances in Engineering Software, vol. 35, no. 3–4, pp. 129–137, 2004, doi: 10.1016/j.advengsoft.2004.03.005.

[8] A. Khaled, "' HVLJQ RI D UREXVW 3 ,' FRQWUROOHU XVHG LQ 39 V \ VWHPV," no. 1, pp. 370–375, 2020.

[9] C. T. Chao, N. Sutarna, J. S. Chiou, and C. J. Wang, "An optimal fuzzy PID controller design based on conventional PID control and nonlinear factors," Applied Sciences (Switzerland), vol. 9, no. 6, 2019, doi: 10.3390/app9061224.

[10] B. Saleh et al., "Design of PID Controller with Grid Connected Hybrid Renewable Energy System Using Optimization Algorithms," Journal of Electrical Engineering and Technology, vol. 16, no. 6, pp. 3219–3233, 2021, doi: 10.1007/s42835-021-00804-7.

Research Article

[11] V. P. Vinod and A. Singh, "A Comparative Analysis of PID and Fuzzy Logic Controller in an Autonomous PV-FC Microgrid," 2018 International Conference on Control, Power, Communication and Computing Technologies, ICCPCCT 2018, pp. 381–385, 2018, doi: 10.1109/ICCPCCT.2018.8574237.

[12] A. A. A. El-ela, A. E. Helal, and R. A. Amer, "ISSN : 1110-1180, ERJ Faculty of Engineering Menoufia University Controller Design to Enhance the Performance of a DC Microgrid Containing Solar PV Connected to the Main Grid Department of Electrical Eng ., Shebin Elkom Faculty of Eng ., Me," vol. 46, no. 3, pp. 283–288, 2023.

[13] D. Panda, P. Kundu, and B. S. Rajpurohit, "Weak Gird Control using Globally Non-overshooting/ Undershooting Controller," 10th IEEE International Conference on Power Electronics, Drives and Energy Systems, PEDES 2022, pp. 1–5, 2022, doi: 10.1109/PEDES56012.2022.10080287.

[14] H. Cha, T. K. Vu, and J. E. Kim, "Design and control of proportional-resonant controller based Photovoltaic power conditioning system," 2009 IEEE Energy Conversion Congress and Exposition, ECCE 2009, no. June 2015, pp. 2198–2205, 2009, doi: 10.1109/ECCE.2009.5316374.

[15] M. Tahmid Wara Ucchas, M. Mustafiz Nuhas, M. Toufiquzzaman, A. Jaber Mahmud, and M. Fokhrul Islam, "Performance and Comparative Analysis of PI and PID Controller-based Single Phase PWM Inverter Using MATLAB Simulink for Variable Voltage," 2022 2nd International Conference on Advances in Electrical, Computing, Communication and Sustainable Technologies, ICAECT 2022, pp. 1–6, 2022, doi: 10.1109/ICAECT54875.2022.9807857.

[16] S. Rhili, H. Trabelsi, and J. Hmad, "PI and PR Current Controllers of Single Phase Grid Connected PV system : Analysis, Comparaison and Testing," 16th International Multi-Conference on Systems, Signals and Devices, SSD 2019, pp. 700–705, 2019, doi: 10.1109/SSD.2019.8893232.

[17] O. Noureldeen and A. M. A. Ibrahim, "Modeling, implementation and performance analysis of a grid-connected photovoltaic/wind hybrid power system," Proceedings of 2018 International Conference on Innovative Trends in Computer Engineering, ITCE 2018, vol. 2018-March, pp. 296–304, 2018, doi: 10.1109/ITCE.2018.8316641.

[18] P. Kumar Hota, "Fault Analysis of Grid Connected Photovoltaic System," American Journal of Electrical Power and Energy Systems, vol. 5, no. 4, p. 35, 2016, doi: 10.11648/j.epes.20160504.12.